Journal of the Korean Nuclear Society
Volume 36, Number 2, pp.165~174, April, 2004

Wire-wrap Models for Subchannel Blockage Analysis

K.S. Ha, H.Y. Jeong, W.P. Chang, Y.M. Kwon, and Y.B. Lee
Korea Atomic Energy Research Institute
150 Deokjin-dong, Yuseong-gu, Daejeon, 305-353, Korea
ksha@kaeri.re.kr

(Received December 19, 2003)

Abstract

The distributed resistance model has been recently implemented into the MATRA-LMR code in order to improve its prediction capability over the wire-wrap model for a flow blockage analysis in the LMR. The code capability has been investigated using experimental data observed in the FFM (Fuel Failure Mock-up)-2A and 5B for two typical flow conditions in a blocked channel. The predicted results by the MATRA-LMR with a distributed resistance model agreed well with the experimental data for wire-wrapped subchannels. However, it is suggested that the parameter n in the distributed resistance model needs to be calibrated accurately for a reasonable prediction of the temperature field under a low flow condition. Finally, the analyses of a blockage for the assembly of the KALIMER design are performed. Satisfactory results by the MATRA-LMR code were obtained through and rerified a comparison with results of the SABRE code.

Key Words : liquid metal reactor, flow blockage, wire-wrap model, wire forcing function model, distributed resistance model, MATRA-LMR, KALIMER

1. Introduction

In a liquid metal reactor (LMR), the core coolant channels could be blocked by obstacles made of either foreign materials remaining in the primary coolant system or degraded fuel itself, as acesult of a compact core design. The flow disturbance around the blockage may cause fuel pin damage due to a reduced local cooling capability. The single pin damage then could propagate to other fuel pins and eventually initiate a severe core disruptive accident. Thus, a flow channel blockage is of concern in a LMR. To prevent or mitigate the set of circumstances leading to a serious consequence, it is required to predict the temperature distributions within an assembly containing a flow blockage channel using a reliable computer code applicable to the situation. Experimental observations of the flow in wire wrapped bundles indicate that the wire wraps not only increase the overall pressure drop in the bundle, but also divert the flow locally in the direction of the wraps. The flow resistance of the wire-wrap is known to be a key factor affecting the

code prediction for the phenomenon.

MATRA-LMR[1], a subchannel analysis code, has been developed for the analysis of the thermal-hydraulics of the LMR core, where design limits are imposed on the maximum temperatures of the cladding and the fuel pins. The objective of this study is to improve the prediction capability of the MATRA-LMR for the coolant temperature distribution during a subchannel blockage of a wire-wrapped rod bundle. Both the 'forcing function model' and 'distributed resistance model' are examined. In the forcing function model, the flow is redirected locally along the path of the wire-wrap and the axial friction factor is distributed uniformly everywhere. The forcing function model is based only on continuity considerations and does not account for the momentum effects. On the other hand, the distributed resistance model adds resistance terms to both the axial and lateral momentum equations under an assumption that the effect of a wire-wrap can be represented solely by its direction and resistance characteristics. Because preliminary analysis results show that the former model does not fully describe the actual flow behaviors observed in the experiments, the latter is now being examined to reduce the uncertainties involved in the forcing function model.

Davis et al.[2] developed a distributed resistance model for the SABRE subchannel analysis code for predominantly axial flows under turbulent flow conditions. Ninokata et al.[3] extended the model to a predominantly lateral flows. In Ninokata's model, a laminar flow condition was also considered. To cover wider flow conditions, Ninokata's model in the following section has been implemented into the MATRA-LMR. Several simulations have been performed to determine some parameters for two non-blockage experiments, before the code is applied to the two flow blockage experiments for validation.

To evaluate the applicability of the MATRA-LMR code with the distributed resistance model, calculation results using the MATRA-LMR for blockages of the assembly of KALIMER(Korea Advanced Liquid Metal Reactor), which is a sodium cooled pool-type reactor with a thermal output of 392.0 MWt, have been compared with the results of the SABRE.

2. Distributed Resistance Model

2.1. Application of DRM

The MATRA-LMR code has two numerical schemes. One is an implicit scheme solving a problem by the MARCHING method and the other is an explicit scheme by both the ACE method and donor cell method to compute the convective quantities [4]. The implicit scheme is not appropriate for the analysis of a flow blockage, because of the inconsistency between the solving procedure and flow direction. In this study, focus is mainly placed on the explicit scheme and the axial and lateral momentum balance equations for a subchannel are as follows;

$$\frac{\partial}{\partial t}\langle \rho u\rangle_{\nu} A+\frac{\partial}{\partial X}\langle \rho u^2\rangle_{A} A+\{D_C^T\}\langle \rho uv\rangle_{S} S = -A\frac{\partial}{\partial X}\langle p\rangle_{A}-A\langle \rho\rangle_{A} g-C_T\{D_C^T\}[w'][D_C]\{u'\} - \frac{1}{2}\left(\frac{f}{D_h}+\frac{K}{\Delta X}\right)\langle \rho u^2\rangle_{A} A \quad (1)$$

$$\frac{\partial}{\partial t}\langle \rho v\rangle_{v'} S+\frac{\partial}{\partial X}\langle \rho vu\rangle_{A'} S+C_S\{D_C\}\{D_C^T\}\left\{\frac{S}{l}\langle \rho v^2\rangle_{S}\cos\beta\right\} = -\frac{S}{l}\{D_C\}\{\langle p\rangle_{A}\}-\frac{1}{2}\frac{S}{l}K_G\langle \rho v^2\rangle_{S} \quad (2)$$

where β is the angle of a communicating gap and the gap of interest.

The last terms of the right-hand side of eqns. (1) and (2) represent the momentum exchange between the solid surface and the fluid. These

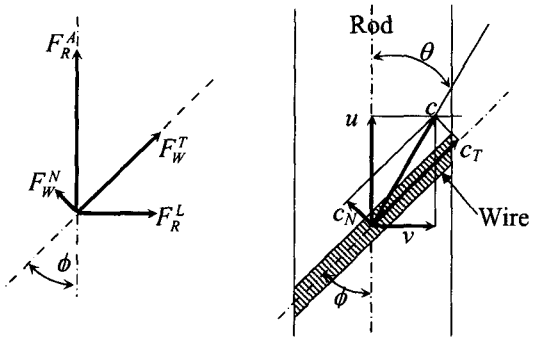

Fig. 1. Components of the Drag Forces and Velocities in a Wire-wrapped Rod

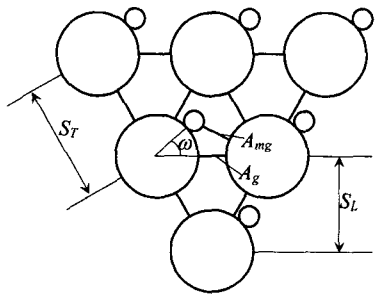

Fig. 2. Averaged Wire-wrap Position and Gap Definition

terms, which are the forces exerted on the fluid by the wall, are replaced with the distributed resistance terms developed by Ninokata et al.. These terms for the rod bundles with wire-wraps can be divided into four components, as shown in Fig. 1. The forces of F_R^L and F_W^N are estimated by correlations depending on the direction of the dominant flow. Each force can be written as:

$$F_R^A = \frac{A_R f}{8}\rho c|c|\cos\theta \tag{3}$$

$$F_W^T = \frac{A_W f}{8}\rho c|c|\cos(\phi-\theta) \tag{4}$$

- Predominantly lateral flow

$$F_R^L = \frac{A_R f}{8}\rho v|v|\left(\frac{D_V''}{S_T}\right)^{0.4}\left(\frac{S_L}{S_T}\right)^{0.6}\frac{1}{E(\omega)} \tag{5}$$

$$F_W^N = \frac{A_W f}{8}\rho v_N|v_N|\left(\frac{D_V''}{S_T}\right)^{0.4}\left(\frac{S_L}{S_T}\right)^{0.6}\frac{1}{E(\omega)} \tag{6}$$

- Predominantly axial flow

$$F_R^L = \frac{A_W'' f}{8}\rho v|v|\left(\frac{D_V''}{S_T}\right)^{0.4}\left(\frac{S_L}{S_T}\right)^{0.6} \tag{7}$$

$$F_W^N = \frac{A_{wp} f_n}{2}\rho v_N|v_N| \tag{8}$$

$$f_n = \left(\frac{A_g}{A_{mg}}\right)^n\left[1+\frac{10}{\mathrm{Re}^{0.667}}\right] \tag{9}$$

where $c^2=u^2+v^2$, A_R, A_W, and A''_W are the surface areas of the rod, wire-wrap, and the total of a control volume, respectively. The f variables dente mean the friction factors, which are estimated using the appropriate correlations. In the case of a lateral flow, the Gunter-Shaw correlation [5] is introduced with the multiplication factor E(ω) given by Suh *et al.* [6]. D''_V is the volume averaged hydrodynamic diameter,. $D''_V = 4\Delta V_f / A''_W$. v_N, which is defined as $v_N=u\sin\phi - v\cos\phi$, and is the normal velocity on the wire-wrap direction. S_T is the rod pitch and S_L is the distance between the two rods in a transverse row (Fig. 2). A_{wp} is the frontal area of the wire-wrap. A_g is the gap flow area and A_{mg} is the minimum gap flow area, as defined in Fig. 2. The exponent n of Eq. (9) has a different value according to the type of subchannel or gap control volume. The four forces above are divided into vertical and horizontal directions and applied to eqns. (1) and (2):

$$\frac{1}{2}\left(\frac{f}{D_h}+\frac{K}{\Delta X}\right)\langle\rho u^2\rangle_A A = \frac{1}{\Delta X}\left\{\frac{A_R f}{8}\rho c|c|\cos\theta + \frac{A_W f}{8}\rho c|c|\cos(\phi-\theta)\cos\phi + F_W^N\sin\phi\right\} \tag{10}$$

$$\frac{1}{2}\frac{S}{l}K_G\langle\rho v^2\rangle_S = \frac{1}{l\Delta X}\left\{F_R^L + \frac{A_W f}{8}\rho c|c|\cos(\phi-\theta)\sin\phi - F_W^N\cos\phi\right\} \tag{11}$$

Eqns. (10) and (11) were numerically implemented into the MATRA-LMR code. In general, if the forces above are treated as source terms, they increase the cross flows due to the wire-wrap; however, the time step is limited by it. If they are treated as the coefficients of the new time velocities, they increase the numerical stability while the cross flow decreases. The explicit solution scheme of the MATRA-LMR expresses the flow resistances with a semi-implicit scheme using new time velocities to compute the pressure drop. Under these considerations, the third terms inside the brackets of Eqns. (10) and (11) are divided into implicit and explicit parts to yield an appropriate flow field due to the wire-wrap. Referring to other experiments and simulation results, only 10% of the third term has been added to the source terms.

2.2. Benchmark Calculation

Two FFM(Fuel Failure Mockup)-2A experiments [7] without a blockage have been simulated to determine a relevant cross flow by the adjustment of the explicit part of both Eqns. (10) and (11) and by the calibration of the exponent of n. Then, two FFM-5B [8] exponments a blockage plate have been simulated for a benchmark. A schematic diagram for the simulation of the experiments is given in Fig. 3. The test assembly was modeled with 40 subchannels, 60 gaps, and 40 axial levels.

The bundle of the FFM-2A experiments contained 19 simulated fuel rods in a hexagonal duct and all the rods were arranged in a triangular pitch. Each rod was 5.842 mm in diameter, and the diameter of the wire spacers was 1.4224 mm. The configuration consisted of a 304.8 mm entrance length, followed by a 533.4 mm heated section with a 152.4 mm exit region.

In the high flow and high power case, the power from the heated section is 16.975 kW/rod and

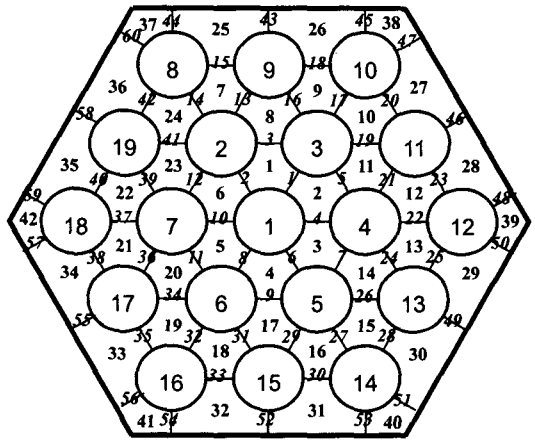

Fig. 3. Subchannel and Gap Numbering for the MATRA-LMR

the flow rate at the inlet is 3.0378 kg/s (55 gal/min). In the low flow and low power case, the power is 0.263 kW/rod and the flow rate is 0.04087 kg/s (0.15 gal/min). The outlet temperatures predicted using the distributed resistance model are compared with those using the wire-forcing function in Fig. 4. The value of the exponent n is tuned to be 1.0 for the inner control volumes of the gaps and channels, 4.5 for the edge control volumes, and 3.0 for the outer control volumes throughout the two runs. Large values for the edge and outer regions are allocated to generate a swirl flow at the edge, which is a representative characteristic of a wire-wrapped channel. The calculation results using both the wire-forcing function model and the distributed resistance model agree well with the experiments without a blockage. Therefore, the application of the distributed resistance model to the MATRA-LMR code is considered successful.

The prediction capability of the code with the distributed resistance model for a flow blockage analysis has been assessed using experiments conducted in a FFM-5B test bundle. In the experiments about one-third of the flow area was blocked at the edge around the corner

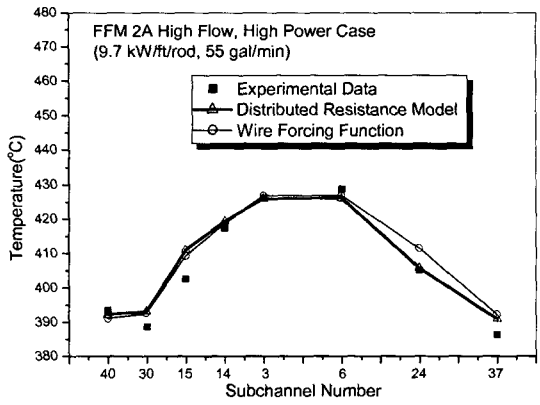

(a) The case of high flow and high power

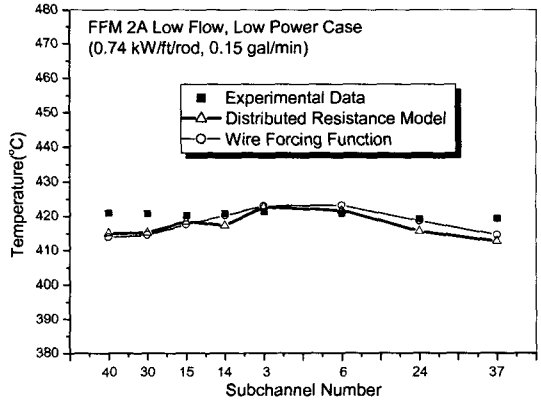

(b) The case of low flow and low power

Fig. 4. MATRA-LMR Predictions for the Experiment Without a Blockage

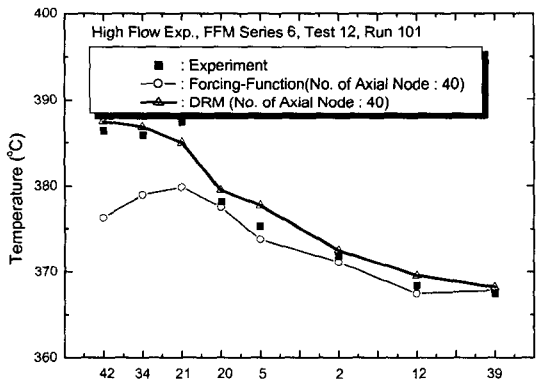

(a) The case of high flow and high power

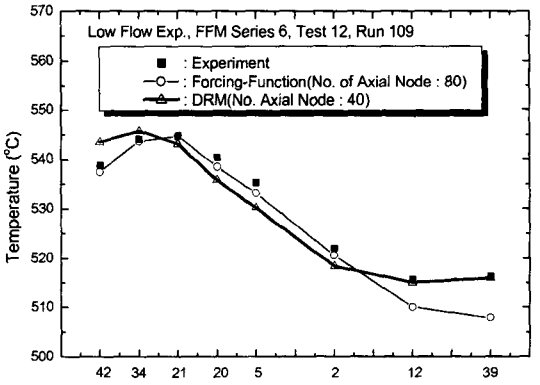

(b) The case of a low flow and low power

(a) The case of a high flow and a high power

(b) The case of a low flow and a low power

Fig. 5. MATRA-LMR Predictions for the Experiment with a Blockage

subchannels, 37, 42, and 41 in Fig. 3. The inlet temperature was 323.6℃ and the inlet velocity was 6.93 m/s. The total heat input from the 19 rods was 145 kW, equivalent to 90.9 W/cm^2/rod [8]. When some part of the flow path was blocked, the downstream temperature of the blockage increased, as shown by the experimental data in (a) of Fig. 5. This mainly arises from the formation of recirculating wakes just above the blockage. In (a) of Fig. 5, it is also seen that the temperature profile in the blocked subchannel is predicted reasonably well with the wire forcing function, whereas the calculated magnitude of the highest temperature is smaller than that of experimental data. Even though the magnitude of the temperature predicted by the distributed resistance model may be closer to the experimental data, the distributed flow resistance model fails to predict the location of the highest temperature. Nevertheless, the overall prediction by the distributed flow resistance model seems to be preferable to the calculation result using the wire forcing function.

MATRA-LMR with the distributed resistance

Table 1. Design Parameters for KALIMER

Core	Core thermal output (MWt)	392.2
	Core electric power (MWe)	150.0
	Core inlet/outlet temperatures (℃)	386.2/530.0
	Total flow rate (kg/s)	2143.1
	Active core height (mm)	1000.0
	Core diameter (mm)	3460.8
	Core configuration	Radial homogeneous
	Pins per fuel assembly (driver)	271
Fuel rod	Total axial height (mm)	3163.0
	Rod outer diameter (driver) (mm)	7.4
	Rod pitch (driver) (mm)	8.9
	Wire wrap diameter (driver) (mm)	1.4
	Wire wrap lead (driver) (mm)	204.9
	Cladding thickness (driver) (mm)	0.55
	Duct wall thickness (mm)	3.7
	Duct inside flat-to-flat distance (mm)	149.6
	Nominal linear pin power (driver) (W/cm)	22.546
	Assembly nominal flow rate (driver) (kg/s)	27.2
	Assembly coolant inlet temperature (℃)	386.2
	Number of axial nodes	103
	Radial power distribution	Uniform

model is now evaluated using the experiment performed under the conditions of a lower inlet velocity and lower heat input. The velocity is 0.48 m/s and the heat input is 52.8 kW. As shown in (b) of Fig. 5, the result using the wire forcing function agrees well with the experimental data except for the data for the opposite side of the blockage plate. On the other hand, the distributed resistance model generally correlates well with all of the data profiles. For the case of a high flow, the MATRA-LMR with the distributed resistance model also fails to predict the location of the highest temperature. This result leads to the conclusion that the distributed resistance model should be calibrated more precisely. In the boundary between the high velocity region and the low velocity region, depending on the local Reynolds or Peclet number, such as the wake boundary, the numerical diffusion could induce a serious problem when upwind differencing is used. In this regard, another deviation from the experimental data in the low flow region might arise from the unrealistic numerical representation for the convective terms. It has been proposed that this numerical diffusion could be avoided by the use of hybrid differencing or vector upwind differencing [9].

2.3. Application to the Blockage of the Assembly of KALIMER

The Korea advanced liquid metal reactor (KALIMER), a 150 MWe pool type sodium cooled prototype reactor, has been completed to its preliminary design stage. The KALIMER core system is designed to generate 392.2 MWt of power. The reference core utilizes a homogeneous core configuration in the radial direction with two driver fuel enrichment zones, surrounded by a layer of blanket assemblies. The reference core

has an active core height of 100 cm and a radial equivalent diameter of 172 cm, and the height-to-diameter ratio for the active core becomes 0.581. The physically outermost core diameter of all the assemblies is 344.7 cm. The major design parameters and geometric characteristics of the assembly are given in Table 1.

A KALIMER driver fuel assembly was chosen to calculate the temperature distribution with the MATRA-LMR and to compare the results with the SABRE code. Fig. 6 shows the subchannel numbers where the temperatures were compared across the assembly.

The effects of blockages on reactor safety depend on several factors such as the size and thermophysical properties of the blockage, location of the blockage in the assembly, fuel pin power, and the coolant velocity in the assembly. In this paper, the area and radial location of the blockage were considered. The areas are a 6-channel blockage, 24-channel blockage, and 54-channel blockage; and the locations are the center, mid-point, and edge, as shown in Fig. 6. Nine calculations were performed at a uniform pin power of 22.546 W/cm with a mean coolant velocity of about 5.5 m/s, which represents the design operation conditions of the driver fuel assembly of KALIMER.

Fig. 7 shows the typical sodium temperature profiles at the just above the blockage and the exit for a 6-channel center blockage. The temperature predictions along the axial level are very similar; however, the results of the SABRE are slightly higher than those of the MATRA-LMR. These trends are observed in all the simulations except for the calculation of the 54-channel blockage. As shown in Fig. 8, the two code results are in good agreement for the 6-channel blockage and 24-

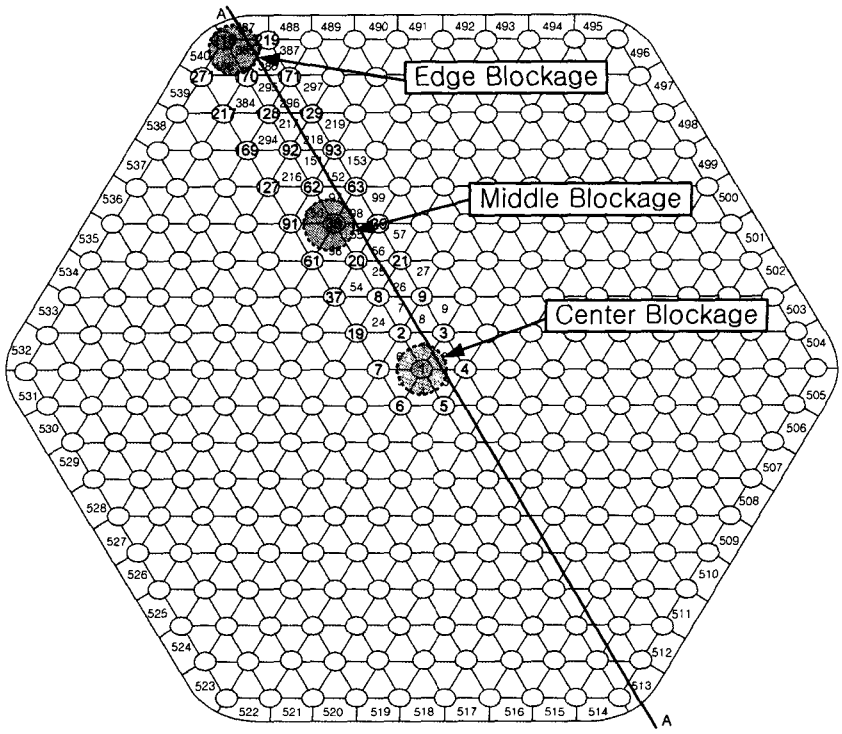

Fig. 6. MATRA-LMR 217 Pins Subchannel Numbering Scheme

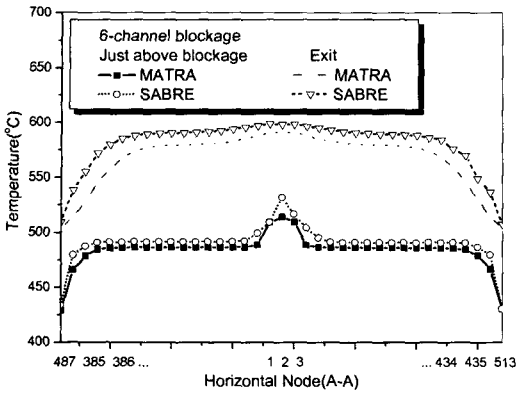

Fig. 7. The Comparison of the Temperature Profiles

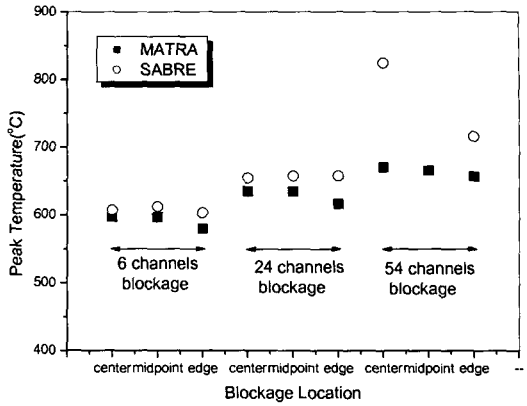

Fig. 8. The Comparison of the Peak Temperatures

channel blockage. In the simulation of the 54-channel blockage, the recirculation region was larger in the calculations by the SABRE than by the MATRA-LMR. This is mainly due to the difference in the numerical scheme of the two codes. The SABRE code basically treats the convective terms with upwind differences. If the magnitude of the Peclet or Reynolds number is less than 2 then a central difference is applied. This causes an increase in the residence time of the sodium coolant in the recirculation region of the blockage downstream. For reference, blockage investigations, which simulated the German Sodium-cooled fast Reactor (SNR), showed the peak temperature was about 780℃ for the blocked fraction of 0.147 of the total flow area in the conditions of an inlet temperature of 380℃ and a mass flow rate of 23 kg/s, similar to the specification of KALIMER design[10]. The SABRE code computed the peak temperature to be 824℃ and the MATRA-LMR code calculated a temperature of 671℃ for the blocked fraction for a 54-channel blockage of 0.09. It might be concluded that the MATRA-LMR gives more precise predictions than the SABRE for these cases.

3. Conclusions

A subchannel analysis code, MATRA-LMR, with the distributed resistance model has been evaluated to improve the capability to predict the coolant temperature in a blocked subchannel in a LMR. The local blockage in a subassembly of a LMR is of particular importance, because local sodium boiling resulting from a flow stagnation in the downstream of the blockage could not only threaten the integrity of both the fuel and the clad, but also affect the core reactivity feedback. Upon this background, the distributed resistance model has been implemented into the MATRA-LMR for the analysis of a flow blockage of a LMR in the present study. The MATRA-LMR with the distributed resistance model has been assessed using the ORNL 19-pin FFM 5B bundle test for high inlet velocity and high heat addition, 6.93 m/s and 145kW, respectively. Another calculation has also been performed for a low inlet velocity of 0.48 m/s and low heat input of 52.8 kW. The simulated results with the distributed resistance model have generally shown good agreement with the experimental data compared to the results with the wire forcing function. Nevertheless, some discrepancies have also been found with the

experimental data in the subchannels after the blockage. From the benchmark calculations, it is suggested that the parameter n needs to be calibrated more accurately to predict a reasonable temperature field under the condition of a low flow. In the application for the assembly of the KALIMER design, the MATRA-LMR has produced comparable results to the SABRE code. From the above calculations and through more validation calculations in the future, the MATRA-LMR code will be improved such that it can be used as a reliable analysis tool for the accident of a flow blockage.

Nomenclature

A = Averaged area of two axial level
$[D_c]$ = Matrix for interchannel connection
$E(\theta)$ = cross flow resistance factor for the wire wrap position from a reference gap
f = Friction factor in rod bundle without wire wrap
K = Form loss coefficient
l = Distance between the center of two adjacent subchannels
p = Pressure
S = Gap width
S_L = Rod pitch
S_T = Distance between two rods in a transverse row
u = Axial velocity
v = Transverse velocity or specific volume
ΔX = Axial node size
A_R = Rod surface area
A_W = Wire-wrap surface area within a control volume
F_R^A = Axial component of the force exerted by the rod surface
F_R^L = Lateral component of the force exerted by the rod surface
F_W^T = Tangential component of the force exerted by the wire-wrap surface
F_W^N = Normal component of the force exerted by the wire-wrap surface
ϕ = Wire-wrap angle
ω = Wire-wrap position

Acknowledgement

This work has been performed under the nuclear R&D program supported by the Ministry of Science and Technology of the Korean Government.

References

1. Kim, W. S., et al., 2002, A subchannel analysis code MATRA-LMR for wire wrapped LMR subassembly, *Annals of Nuclear Energy*, **29**, 303-321.
2. Davis , A. L. et al., 1979, SABRE I - A computer program for the calculation of three dimensional flows in rod clusters, AEEW-R 1057.
3. Ninokata, H., et al., 1987, Distributed resistance modeling of wire-wrapped rod bundles, *Nuclear Engineering and Design*, **104**, 93-102.
4. Stewart, C. W., et al., 1977, COBRA-IV: The model and the method, BNWL-2214.
5. Gunter, A. Y., and Shaw, W. A., 1945, A general correlation of friction factors of various types of surfaces in crossflow, *Transaction of ASME*, **67**, 643-660.
6. Suh, K. Y., and Todreas, N. E., 1987, An experimental correlation of cross-flow pressure drop for triangular array wire-wrapped rod assemblies, *Nuclear Technology*, **76**, 229-240.
7. Fontana, M. H., et al., 1974, Temperature distribution in the duct wall and at the exit of 19-rod simulated LMFRB fuel assembly.

Nuclear Technology, **24**, 176-200.

8. Domanus, H. M., et al., 1980, Applications of the COMMIX code using the porous medium formulation, *Nuclear Engineering and Design*, **62**, 81-100.
9. Macdougall, J. D. and Lillington, J. N., 1984, The SABRE code for fuel rod cluster thermohydraulics, *Nuclear Engineering and Design*, **82**, 171-190.
10. Kirsch, D., 1974, Investigations on the flow and temperature distribution downstream of local coolant blockages in rod bundle subassemblies, *Nuclear Engineering and Design*, **31**, 266-279.